[9]G. W. Fehrenbach, K. J. Gruntz, and R. G. Ulbrich, Appl. Phys. Lett. **33**, 159 (1978). Subpicosecond pulses in the near IR could also be achieved by using an 80% output mirror without the addition of saturable absorber dyes.
[10]R. H. Stolen and Chinlon Lin, Phys. Rev. A **17**, 1448 (1978).
[11]H. Nakatsuka, D. Grischkowsky, and A. C. Balant, Phys. Rev. Lett. **47**, 910 (1981).
[12]D. Bebelaar, Rev. Sci. Instrum. **50**, 1629 (1979).
[13]E. W. Van Stryland, Opt. Commun. **31**, 93 (1979); S. L. Shapiro, R. R. Cavanagh, and J. C. Stephenson, Opt. Lett. **6**, 470 (1981).

Picosecond carrier dynamics and laser action in optically pumped buried heterostructure lasers

T. L. Koch, L. C. Chiu, Ch. Harder, and A. Yariv
Mail Stop 116-81 California Institute of Technology, Pasadena, California 91125

(Received 15 March 1982; accepted for publication 5 April 1982)

We report the observation of picosecond optical pulses and unusual pulse structures from optically pumped buried heterostructure semiconductor lasers. A model which considers the hot electron and hole energy distributions dynamically accounts well for our experimental findings. The results are relevant to the problem of the limiting response time of semiconductor lasers.

PACS numbers: 42.55.Px, 78.45. + h, 78.20. − e

Over the past several years there has been a continued interest in the generation of picosecond pulses from semiconductor diode lasers. We report here some preliminary results from an experiment to investigate the picosecond carrier and lasing dynamics of high quality buried heterostructure (BH) lasers using techniques similar to those outlined in earlier work with stripe lasers.[1] The GaAs-AlGaAs BH lasers, shown in Fig. 1, were grown in our laboratory with a transparent contact over the active waveguiding region to allow optical pumping as well as the usual electrical operation, and had typical threshold currents in the 20–30-mA range. Electrical operation was required for alignment into the optical measurement system to be described in the following, but was used only for this purpose.

Gigawatt level subpicosecond pulses were generated from a cw synchronously mode-locked dye laser and Nd:yttrium aluminum garnet (YAG) pumped amplifier chain combination at a 10-Hz repetition rate.[2] The tunable system was operated at 598 nm and split into two paths. One was Raman shifted with deuterated acetone to 686 nm and was then focused onto the BH laser, passing through the transparent contact and $Al_{0.4}Ga_{0.6}As$ upper cladding region to be absorbed directly in the active region of the device. The second pulse was sent through a variable delay arm and then combined collinearly with the IR BH laser output in a $LiIO_3$ crystal phase matched for sum frequency generation. The sum frequency was fed into a signal averaging system, effectively synthesizing a slow sweep picosecond resolution sampling oscilloscope by varying the delay of the short amplified dye laser pulse.

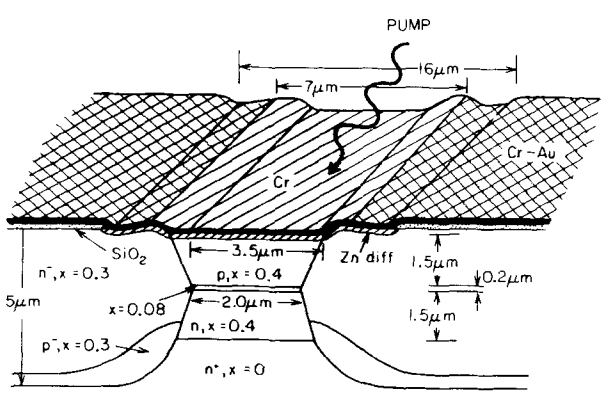

FIG. 1. Geometry of buried heterostructure laser used in experiment.

We find that the picosecond dynamics of optically pumped semiconductor lasers are not as strongly dependent upon the cavity length as has been suggested by other investigators working with thin platelet GaAs and InGaAsP lasers.[3,4] The important quantities for short pulse operation are fast and significant gain/loss transients to initiate laser action and a short photon lifetime for termination. Numerical work also indicates that with reasonable values for distributed losses, calculations employing longitudinally averaged rate equations give results almost identical to those employing bidirectional propagation with longitudinal spatial variations included in the variables, even when the transit time becomes comparable to the output pulsewidth. Figure 2 shows the experimental results from a 200-μm device

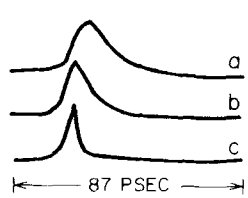

FIG. 2. BH diode laser output; a, b, and c are the long, medium, and short wavelength normalized outputs with pulsewidths of 15.6, 9.0, and 4.5 ps respectively.

 0003-6951/82/010006-03$01.00

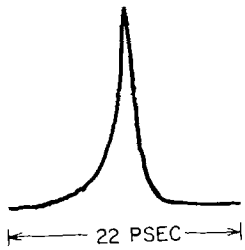

FIG. 3. Short wavelength BH laser output under high pumping conditions. Pulse FWHM is 1.2 ps, and note unusual shape.

which, even at this sizable length, already has a short photon lifetime of ~ 1.3 ps. The four curves are the normalized output at three wavelengths obtained by angle tuning the $LiIO_3$ crystal. The pulse full width at half-maximum (FWHM) are 4.5, 9.0, and 15.6 ps at λ_0, $\lambda_0 + 11$ nm, and $\lambda_0 + 23$ nm, respectively, where $\lambda_0 \approx 743 \pm 20$ nm with the large uncertainty in the reference level due only to the rough calculated absolute calibration of the angle tuning. This confirms the trend towards shorter pulses at higher photon energies[3] which appears to be an essential feature when high carrier densities are injected well above the band gap. We estimate the carrier density here to be $\sim 5 \times 10^{18}$ cm^{-3}, although this figure is only approximate due to the uncertainties of the transparent contact injection scheme.

When the pumping level is increased, the general behavior at a fixed wavelength is a forward shift in time and a shortening of the pulse as expected from a usual transient gain/loss analysis. Using the computer model described below, we estimate the upper limit on the carrier density to be $\lesssim 10^{19}$ cm^{-3} due to a dynamic Burstein–Moss bleaching effect at the pump wavelength in the $Al_{0.08}Ga_{0.92}As$ active region. As the lasers are pumped up to this limit, several interesting features begin to appear. As expected from band filling, shorter wavelength pulses are generated, but the pulses also develop unusual temporal profiles. Figure 3 shows the ~ 700-nm pulse output of an 80-μm-long BH laser on an expanded scale with a FWHM of 1.2 ps. Since this approaches the pump pulsewidth ($\lesssim 1$ ps), the deconvolved BH laser pulse is also probably subpicosecond. Note that the rise time is more gradual than the fall time, in sharp contrast to the usual rate equation predictions of gain/loss switched laser action. At long wavelengths, the pulses are longer to start with, but they begin to acquire a distinct tail as the excitation density increases, even to the point of developing a secondary peak at the longest wavelengths of emission. This is shown in Fig. 4, and note the change in scale.

We have completed a computer solution of integro-differential rate equations which include the broadband nature of the optically pumped semiconductor laser output. The model makes simplifying assumptions while still retaining the essential physics of the device; i.e., we employ all the standard results of parabolic band semiconductor theory, taking into account the central Γ and side L valleys in the conduction band but ignoring the split-off valence band, and assume that the Γ and L electrons are equilibrium Fermi–Dirac plasmas with number densities n_Γ and n_L but the same electron temperature T_e, while the holes are characterized by a number density $p = n_\Gamma + n_L$ and temperature T_h. The plasma temperatures $T_{e,h}$, number densities $n_{\Gamma,L}$, and the spatially averaged signal photon density $\phi(\nu)$ are the dynamic variables, and cooling is given by the usual polar optical phonon emission cooling formula[5] which we modified to include Fermi–Dirac statistics and screening by the large free-carrier density. The $\Gamma \rightarrow L$ intervalley scattering is also included by integrating an easily calculated scattering rate,[5] and temperature equilibration from electron-hole collisions is approximated by standard two-temperature plasma results.[6] The rate equations are

$$\frac{dn_\Gamma}{dt} = -\frac{I_p(t)}{h\nu_p}\alpha(\nu_p,n_\Gamma,p,T_e,T_h) + \left.\frac{dn_\Gamma}{dt}\right|_{\Gamma\rightarrow L} - \int_0^\infty \left(\frac{c}{n}\alpha(\nu,n_\Gamma,p,T_e,T_h)\phi(\nu) + r(\nu,n_\Gamma,p,T_e,T_h)\right)d\nu, \tag{1}$$

$$\frac{dn_L}{dt} = -\left.\frac{dn_\Gamma}{dt}\right|_{\Gamma\rightarrow L} \tag{2}$$

$$\frac{d\phi(\nu)}{dt} = \left(\Gamma\frac{c}{n}\alpha(\nu,n_\Gamma,p,T_e,T_h)\phi(\nu) + \beta r(\nu,n_\Gamma,p,T_e,T_h)\right) - \phi(\nu)/\tau_{ph}, \tag{3}$$

$$\frac{dT_e}{dt} = \frac{1}{(\partial U_e^\Gamma/\partial T_e + \partial U_e^L/\partial T_e)} \times\left[-\frac{m_r}{m_e}\left(1-\frac{E_g}{h\nu_p}\right)I_p(t)\alpha(\nu,n_\Gamma,p,T_e,T_h) - \frac{m_r}{m_e} \times\int_0^\infty\left(\frac{c}{n}\alpha(\nu,n_\Gamma,p,T_e,T_h)\phi(\nu) + r(\nu,n_\Gamma,p,T_e,T_h)\right)h\nu\,d\nu - \Delta\left.\frac{dn_\Gamma}{dt}\right|_{\Gamma\rightarrow L} + \left.\frac{dU_e^\Gamma}{dt}\right|_{\text{phonon cool}} + \left.\frac{dU_e^L}{dt}\right|_{\text{phonon cool}} + \left.\frac{d(U_e^\Gamma+U_e^L)}{dt}\right|_{e-h\text{ collisions}} - \frac{\partial U_e^\Gamma}{\partial n_\Gamma}\frac{dn_\Gamma}{dt} - \frac{\partial U_e^L}{\partial n_L}\frac{dn_L}{dt}\right], \tag{4}$$

$$\frac{dT_h}{dt} = \frac{1}{\partial U_h/\partial T_h} \times\left[-\frac{m_r}{m_h}\left(1-\frac{E_g}{h\nu_p}\right)I_p(t)\alpha(\nu,n_\Gamma,p,T_e,T_h) - \frac{m_r}{m_h} \times\int_0^\infty\left(\frac{c}{n}\alpha(\nu,n_\Gamma,p,T_e,T_h)\phi(\nu) + r(\nu,n_\Gamma,p,T_e,T_h)\right)h\nu\,d\nu + \left.\frac{dU_h}{dt}\right|_{\text{phonon cool}} - \left.\frac{d(U_e^\Gamma+dU_e^L)}{dt}\right|_{e-h\text{ collisions}} - \frac{\partial U_h}{\partial p}\frac{dp}{dt}\right]. \tag{5}$$

Here $I_p(t)$ is the pump intensity, $U_i = U_i(n_i,T_i)$ is the energy density of plasma type i, E_g is the direct energy gap, Δ is the

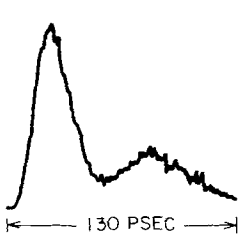

FIG. 4. Long wavelength BH laser output under high pumping conditions. Primary peak of pulse has a 21.6-ps FWHM, but note the secondary peak.

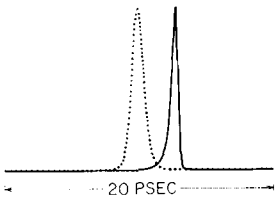

FIG. 5. Computed response of semiconductor laser at short wavelength under high pumping conditions; dotted line is normalized pump pulse shown for time reference. Shape is similar to observed behavior shown in Fig. 3.

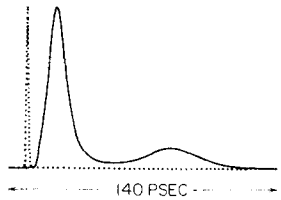

FIG. 6. Computed response of semiconductor laser at long wavelength under high pumping conditions; dotted line is normalized pump pulse shown for time reference. Shape is similar to observed behavior shown in Fig. 4.

energy separation of the L and Γ valley minima, m_e,m_h, and m_r are the electron, hole, and electron-hole reduced masses, respectively, τ_{ph} is the photon lifetime, β is the fraction of spontaneous emission into the lasing modes, and Γ is the mode confinement factor, while the gain/loss $\alpha(\nu,n_\Gamma,p,T_e,T_h)$, recombination rate $r(\nu,n_\Gamma,p,T_e,T_h)$,$\partial U_i/\partial T_i$, and $\partial U_i/\partial n_i$ are all well known expressions involving Fermi–Dirac distributions and integrals involving these distributions.

This relatively simple model predicts almost all of the observed features of the short pulse laser performance. In particular, the strong λ dependence of the pulsewidth is correctly predicted, even in detail down to the unusual shapes as shown in Fig. 3. The important physical effects seem to arise just from the cooling of the plasma and the downward motion of the Fermi levels. After a preliminary cooling period of a few picoseconds the gain is sufficient over a broad range of wavelengths for stimulated emission to begin. An unusual and perhaps nonintuitive computed result is that the lasing actually reheats the plasma due to the preferential elimination of lower energy carriers. This reduces the gain and lasing action slowly or subsides and the plasma then cools again. This mechanism in itself could lead to shoulders on the long wavelength pulses and actually produce double peaks on a picosecond time scale if the cooling were slower than the theoretically predicted value. We have concluded that a more likely mechanism responsible for these secondary peaks is a many-valley effect and consequently this is also included in Eqs. (1)–(5). Because of the high density of states in the L valleys, electrons are rapidly scattered there during the initial excitation when the plasma is still hot and the Γ valley fermi level is high. After lasing has virtually emptied the central Γ valley, the L valley electrons return slowly because of the low density of states in the Γ valley. Here they cool to the band edge to allow the long wavelength emission to continue. Figures 5 and 6 show the computed normalized pulse shapes from the system of equations outlined above at short and long wavelength (~ 67 and ~ 8 nm shorter than the band edge wavelength, respectively) under high pumping conditions (~ 0.15-mJ/cm^2 incident onto the active region). The overall agreement with the observed behavior is seen to be quite good. At lower pumping levels the long wavelength secondary peaks are not present, again in agreement with experiment. The only constant in the calculation which is not well known is the deformation potential for intervalley scattering. The value used was 1.5×10^8 eV/cm which is in the same range as values successfully employed in Gunn effect calculations,[5] but the model is not extremely sensitive to this parameter.

Since any ultrashort pulse driving scheme for semiconductor diode lasers without optical feedback involves large gain and carrier population transients, the phenomena observed here, especially the carrier reheating effects, could play a role under other injection schemes as well and could affect the ultimate short pulse performance of semiconductor lasers.

In conclusion, we have used picosecond spectroscopic techniques to observe some novel picosecond laser dynamics in high quality BH laser structures. We also have shown that a relatively simple hot-carrier model which allows for broadband stimulated emission and intervalley scattering accounts for most of the observed features of our experiment.

This work was supported by grants from the National Science Foundation and the Air Force Office of Scientific Research.

[1]T. L. Koch, D. P. Wilt, and A. Yariv, "*Q*-Switching of Semiconductor Lasers with Picosecond Light Pulses," in *Picosecond Phenomena II*, Springer Series in Chemical Physics, Vol. 14, edited by R. Hochstrasser, W. Kaiser, and C. V. Shank (Springer, Berlin, Heidelberg, New York, 1980), p.34.
[2]T. L. Koch, L. C. Chiu, and A. Yariv, Opt. Commun. **40**, 364 (1982).
[3]T. C. Damen, M. A. Duguay, J. Shah, J. Stone, J. M. Wiesenfeld, and R. A. Logan, Appl. Phys. Lett. **39**, 142 (1981).
[4]J. Stone, J. M. Wiesenfeld, A. G. Dentai, T. C. Damen, M. A. Duguay, T. Y. Chang, and E. A. Caridi, Opt. Lett. **6**, 534 (1981).
[5]E. M. Conwell, *High Field Transport in Semiconductors*, Suppl. 9 in Solid State Physics Series, edited by F. Seitz, D. Turnbull, and H. Ehrenreich (Academic, New York, 1967).
[6]G. Schmidt, *Physics of High Temperature Plasmas*, second ed. (Academic, New York, 1979).